Design for Disassembly With High-Stiffness Heat-Reversible Locator-Snap Systems

Mohammed Shalaby
e-mail: mshalaby@umich.edu

Kazuhiro Saitou[1]
e-mail: kazu@umich.edu

Department of Mechanical Engineering,
University of Michigan,
Ann Arbor, MI 48109-2125

Recent legislative and social pressures have driven manufacturers to consider effective part reuse and material recycling at the end of product life at the design stage. One of the key considerations is to design and use joints that can disengage with minimum labor, part damage, and material contamination. This paper presents a unified method to design a high-stiffness reversible locator-snap system that can disengage nondestructively with localized heat, and its application to external product enclosures of electrical appliances. The design problem is posed as an optimization problem to find the locations, numbers, and orientations of locators and snaps as well as the number, locations, and sizes of heating areas, which realize the release of snaps with minimum heating area and maximum stiffness while satisfying any motion and structural requirements. The screw theory is utilized to precalculate a set of feasible orientations of locators and snaps, which are examined during optimization. The optimization problem is solved using the multi-objective genetic algorithm coupled with the structural and thermal finite element analysis. The method is applied to a two-piece enclosure of a DVD player with a T-shaped mating line. The resulting Pareto-optimal solutions exhibit alternative designs with different trade-offs between the structural stiffness during snap engagement and the area of heating for snap disengagement. Some results require the heating of two areas at the same time, demonstrating the idea of a lock-and-key.
[DOI: 10.1115/1.2991134]

1 Introduction

Recent legislative and social pressures have driven manufacturers to take responsibilities for reducing the amount of materials that end up in the waste stream at product retirement. As such, products are now designed with increased emphasis on the effective part reuse and material recycling at the end of product life using design for disassembly (DFD) [1–4] guidelines. One of the key considerations in DFD is the design and use of joints that can disengage with minimum labor, part damage, and material contamination.

Reversible snaps, often found at battery covers in electrical appliances, are good candidates for such joints. They allow easy, nondestructive, and clean detaching between mating parts at a desired time. However, these snaps are prone to accidental disengagement since they must sacrifice stiffness for the ease of disengagement (Fig. 1(*b*)). Accidental disassembly of electric appliances puts a hazard of electric shock, especially in kitchen appliances as they usually work in damp environments and in electronic devices, which have small capacitors that store huge electric charges. Also, when snaps are used in an external product enclosure, the aesthetic appeal of the product can be damaged due to the exposure of the joint features to which the unlocking force needs to be applied (Figs. 1(*c*) and 1(*d*)).

Accordingly, the objective of this paper is to present a unified method for designing a high-stiffness reversible locator-snap system that can be disengaged nondestructively with localized heat and to show its application to the external product enclosures of electrical appliances. The proposed heat-reversible locator-snap system consists of locators and snaps molded on the internal surfaces around the mating line of a thin-walled enclosure part. While assembled, the locators and the snaps, respectively, engage with the protrusions and the catches molded on the mating part, thereby constraining their relative motions. During assembly, the elasticity of the thin-walled parts is exploited to enable the snapping action. During disassembly, the in-plane thermal expansion constrained by locators and the temperature gradient along the wall thickness are exploited to realize the out-of-plane bulging of the enclosure wall that releases the snaps.

The design problem of the high-stiffness heat-reversible locator-snap system is posed as an optimization problem to find the locations, numbers, and orientations of locators and snaps as well as the number, locations, and sizes of a heating area, which realize the release of snaps while minimizing the heating area, maximizing the stiffness, and satisfying any motion and structural requirements. The screw theory [6] is utilized to precalculate a set of feasible orientations of locators and snaps that are examined during optimization. The optimization problem is solved using the multi-objective genetic algorithm (MOGA) [7,8] coupled with the structural and thermal finite element analysis (FEA). The method is applied to a two-piece enclosure of a DVD player with a T-shaped mating line. The resulting Pareto-optimal [7] locator-snap systems exhibit snap disengagement with a small heating area and sufficient stiffness to withstand its own weight. Some results require simultaneous heating of two areas, demonstrating the idea of a lock-and-key. The lock-and-key concept is like a security code that allows easy disassembly when the right procedure is followed. In this case, it is achieved by heating two locations simultaneously; otherwise, snaps will remain locked.

2 Related Work

2.1 Analysis and Design of Snap Fits. Snap fit is a preferred joining method for the design for disassembly because it does not need extra parts for joining, allows for easy assembly, and can be made cleanly separable, all of which contribute to the reduction of overall product cost and realization of economic recycling pro-

[1]Corresponding author.

Contributed by the Design for Manufacturing Committee of ASME for publication in the JOURNAL OF MECHANICAL DESIGN. Manuscript received November 18, 2007; final manuscript received June 14, 2008; published online November 6, 2008. Review conducted by Jeffrey Herrmann. Paper presented at the ASME 2007 Design Engineering Technical Conferences and Computers and Information in Engineering Conference (DETC2007), Las Vegas, NV, September 4–7, 2007.

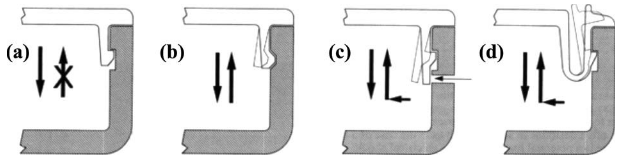

Fig. 1 Different snap-fit types: (*a*) nondisassemblable and disassemblable snaps, (*b*) prone to accidental disassembly, and ((*c*) and (*d*)) affecting the aesthetic appeal [5]

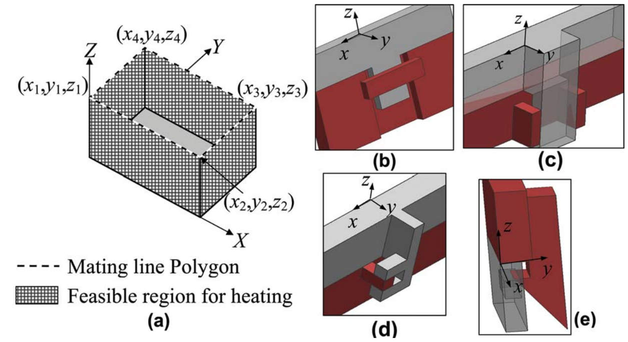

Fig. 2 (*a*) Part geometry (only one part shown), coordinates of vertices of the mating polygon, and feasible region for heating. ((*b*)–(*e*)) Locators and snaps in library.

cesses [9–11]. Early work on integral attachment design focused on the analysis of particular types of locking features such as cantilever hooks [12], bayonet-fingers [13], and compressible hooks [14]. More recently, Genc et al. [15–17] discussed a feature-based method to integral attachment design, which classified snap-fit features into three categories: locating features, locking features, and enhancing features. Luscher et al. [18] discussed a similar classification based on assembly motions. These works, however, did not address the reversible snap-fit designs that are actuated by indirect means such as localized heating.

2.2 Design of Reversible Joints. Chiodo et al. [19] developed the concept of active disassembly using smart materials (ADSM), where heat-induced disassembly is realized by self-disengaging fasteners made of shape memory polymers (SMPs) and compression springs. Li et al. [20–22] reported topology optimization of heat-reversible cantilever snaps, where unsnapping is realized by the local transient thermal deformations of the cantilevers. Although effective in the presented examples, these works have not found many applications due to the need for special, costly, and unstable materials [19] or snaps with impractically small locking surfaces and low stiffness [20–22].

Our previous work [23,24] introduced an initial concept of high-stiffness heat-reversible locator-snap systems that realize nondestructive disassembly of plastic automotive body panels from aluminum frames. Similar to the design concept presented in this paper, it converts the in-plane thermal expansion of a body panel constrained on a rigid frame by locators to out-of-plane bulging large enough to unlock the snap that locks the panel and the frame. However, the concept is specifically developed for assemblies of a semiplanar elastic panel and a rigid frame. Also, the design method discussed in Refs. [23,24] assumes the orientations of locators and snaps given as inputs and only optimizes the numbers and locations of locators and snaps in the given orientations and the area of heating. Since the orientations of locators and snaps largely determine the design's ability to balance elasticity for snap release and stiffness for joint sustaining, the method was incapable of a full exploration of the design space.

The method discussed in this paper generalizes the concept in Refs. [23,24] to be applicable to any thin-walled enclosure assemblies with arbitrary mating lines and extends the design method in Refs. [23,24] to include the orientations of locators and snaps as additional design variables.

2.3 Screw Theory in Motion and Constraint Analysis. The screw theory, a pioneering work by Ball [6], is used for the motion and constraint analysis of rigid bodies. Waldron [25] utilized the screw theory to build a general method to determine all relative degrees of freedom (DOFs) between two rigid bodies making contacts with each other. Extending the work of Konkar and Cutkosky [26], Adams and Whitney [27,28] developed a method to determine the status (overconstrained, underconstrained, or fully constrained) of rigid body assemblies with mating features. Their method also determines the motion type and range of underconstrained rigid body assemblies. Lee and Saitou [29] applied their method to automatically synthesize 3D assemblies with prescribed in-process dimensional adjustability. Our previous work [24] outlined the use of the screw theory to analyze relative motion constraints on a panel and a frame imposed by locators and snaps of given orientations. This approach is applied in this paper to precalculate a set of all feasible orientations of locators and snaps to be examined during optimization.

3 Method

3.1 Overview. The method employed synthesizes the optimal designs of the locator-snap system by solving the following optimization problem:

Given: the geometry of the two mating thin-walled parts, the coordinates of the vertices of the polygon representing the mating line where locators and snaps will be placed, the feasible region for heating, and the library of locators and snaps that can be used.

- Find: locations, numbers, and orientations of locators and snaps as well as number, locations, and sizes of heating areas.
- Minimize: the total heated area to unlock the snaps and the deformation at the mating line under own weight.
- Subject to: The parts are underconstrained and do not interfere with the neighboring parts before snap engagement (ignoring the snaps during the constraint analysis), the parts are not underconstrained and meet any structural requirements after snap engagement (including the snaps during the constraint analysis), local heating induces displacement sufficient for unlocking snaps, and uniform heating does not induce displacement sufficient for unlocking snaps.

Figure 2 shows sample inputs. In addition to the actual geometry of feasible locators (and the associated protrusions) and snaps (and the associated catches) available for a given problem (Figs. 2(*b*)–2(*e*)), the library contains the wrench matrix (obtained as given in Ref. [29]) representing the motion constraints imposed by each locator and snap, with respect to its local coordinate system. For example, the locator in Fig. 2(*b*) constrains the motion in $\pm y$ and $+z$ directions in local coordinates. The locator in Fig. 2(*c*) constrains the motion in $\pm x$ and $+z$ directions in local coordinates. The locator in Fig. 2(*d*) constrains the motion in $\pm z$ directions in local coordinates. Finally, the snap in Fig. 2(*e*) constrains the motion in the $+z$ direction in local coordinates. The optimization problem is solved using a MOGA [7,8] coupled with the structural and thermal finite element analysis.

3.2 Generation of Feasible Orientations of Locators and Snaps. In order to avoid examining a large number of infeasible designs during optimization, a set of all orientations of locators and snaps feasible to the motion constraints of the above optimization problem is precalculated using the screw theory. The following are assumed:

- Locators (and the associated protrusions) and snaps (and the associated catches) can be placed on either of the two mating parts.

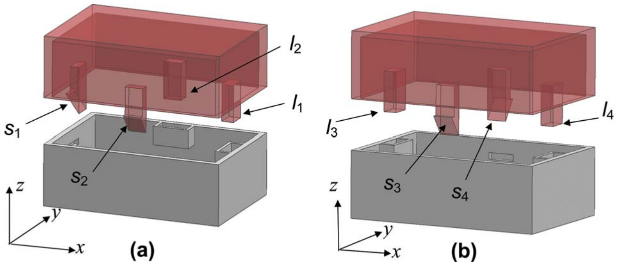

Fig. 3 Examples of two different locator and snap orientations

- Locators (and the associated protrusions) and snaps (and the associated catches) can be placed only at predefined discrete locations (e.g., nodes of finite elements) on the internal surfaces along the edges of the mating polygon and only in predefined discrete orientations (e.g., a subset of 0 deg, 90 deg, 180 deg, and 270 deg) relative to the edge.
- Each edge of the mating polygon can have one or more locators (or the associated protrusions) or snaps (or the associated catches) only of the same type and only in the same orientation.
- Each edge of the mating polygon can have either locators (or the associated protrusion) or snaps (or the associated catch), but not both.

Based on the above assumptions, all possible combinations of locators, snaps, orientations, and edges can be enumerated. Since each edge can only have locators or snaps of the same type in the same orientation, their numbers and locations along each edge can be ignored for the purpose of the analysis of motion constraints. Since relative motion constraints on an edge are independent of the choice of the part (e.g., top or bottom cover) on which the locators or snaps are placed, this choice can also be ignored for the purpose of the analysis of motion constraints. As such, a combination of locators, snaps, orientations, and edges can be represented as

$$\boldsymbol{z} = (c_1, c_2, \ldots, c_n) \tag{1}$$

$$c_i = (l_i, o_i), \quad i = 1, 2, \ldots, n \tag{2}$$

where n is the number of edges in the mating polygon, l_i and o_i are the locator or the snap in the library (nil if no locator/snap) and the orientations among the predefined choices (ignored if l_i = nil), respectively, of the ith edge. Each combination $\boldsymbol{z}$ of locators, snaps, orientations, and edges is tested against two motion constraints in the above optimization problem: (1) the parts are underconstrained and do not interfere with neighboring parts before snap engagement and (2) the parts are not underconstrained (i.e., can be overconstrained) after snap engagement. After testing, only the combinations that satisfy both conditions are stored in a set F of feasible orientations to be examined during optimization.

Examples in Fig. 3 illustrate the two motion constraints. In the figure, it is assumed that a locator can constrain the normal direction (positive and negative) of the surface on which it is placed and its direction of insertion ($-z$ in the figure), a snap can only constrain its direction of disengagement ($+z$ in the figure), and there is no neighboring part that might cause interferences. In the orientations shown in Fig. 3(a), both conditions are satisfied. Locators l_1 and l_2 constrain the motions in the $\pm x$ and $-z$, and $\pm y$ and $-z$ directions, respectively, but nothing constrains the $+z$ direction. After snapping, snaps S_1 and S_2 provide the constraint in this direction, thereby fully constraining the two mating parts. In the orientations shown in Fig. 3(b), on the other hand, the second condition is not satisfied. Locators l_3 and l_4 constrain the motion only in the $\pm x$ and $-z$ directions, whereas snaps s_3 and s_4 constrain the $+z$ direction. The locators are inserted into the constraining boxes, which are wider than the locators in the y direction; thus locators do not constrain the y direction. As a result, this is underconstrained as it is free to move in the $\pm y$ direction.

The above conditions can be more precisely expressed using the screw theory [6]. Adopting the wrench matrix representation similar to Refs. [24,29], for example, the locators and snaps in Fig. 3 are represented as

$$\mathbf{W}_{l_1} = \mathbf{W}_{l_3} = \mathbf{W}_{l_4} = \begin{pmatrix} 1 & 0 & 0 & 0 & 0 & 0 \\ -1 & 0 & 0 & 0 & 0 & 0 \\ 0 & 0 & 1 & 0 & 0 & 0 \end{pmatrix} \tag{3}$$

$$\mathbf{W}_{l_2} = \begin{pmatrix} 0 & 1 & 0 & 0 & 0 & 0 \\ 0 & -1 & 0 & 0 & 0 & 0 \\ 0 & 0 & 1 & 0 & 0 & 0 \end{pmatrix} \tag{4}$$

$$\mathbf{W}_{s_1} = \mathbf{W}_{s_2} = \mathbf{W}_{s_3} = \mathbf{W}_{s_4} = \begin{pmatrix} 0 & 0 & -1 & 0 & 0 & 0 \end{pmatrix} \tag{5}$$

where each row represents the directional (row) vectors of the force and moment in the global reference frame that can be supported by a mating surface in a locator or a snap. For example, the first row in Eq. (3) has −1 at the first column, indicating that the upright surface of locator l_1 can support the force in the $+x$ direction. Note that the moments (the fourth to sixth columns) are ignored due to our primal concern on the translational degrees of freedom. This is justified by using wide locators and snaps. In testing each combination of locators, snaps, orientations, and edges in the enumerated set, the wrench matrix of a locator or a snap placed on an edge in an orientation is transformed to the one with respect to the global reference frame using the rotation matrix constructed from the directional cosines of the edge and the rotation matrix for the orientation.

Based on the principle of virtual work, the forces and moments represented by the wrench matrix $\mathbf{W} = (\boldsymbol{w}_1, \ldots, \boldsymbol{w}_n)^T$ constrain the motions represented by the twist matrix $\mathbf{T} = (\boldsymbol{t}_1, \ldots, \boldsymbol{t}_m)^T$ if and only if there exists a negative component in every column of the virtual coefficient matrix [27],

$$\Delta(\mathbf{W}, \mathbf{T}) = \begin{pmatrix} \delta(\boldsymbol{w}_1, \boldsymbol{t}_1) & \cdots & \delta(\boldsymbol{w}_1, \boldsymbol{t}_m) \\ \vdots & \ddots & \vdots \\ \delta(\boldsymbol{w}_n, \boldsymbol{t}_1) & \cdots & \delta(\boldsymbol{w}_n, \boldsymbol{t}_m) \end{pmatrix} \tag{6}$$

where $s(\boldsymbol{w}, \boldsymbol{t})$ is the virtual coefficient of wrench $\boldsymbol{w} = (\boldsymbol{f}^T, \boldsymbol{m}^T)$ and twist $\boldsymbol{t} = (\boldsymbol{\omega}^T, \boldsymbol{v}^T)$,

$$\delta(\boldsymbol{w}, \boldsymbol{t}) = \boldsymbol{v} \cdot \boldsymbol{f} + \boldsymbol{\omega} \cdot \boldsymbol{m} \tag{7}$$

Equivalently, this can be written as

$$\text{fully constrained}(\Delta(\mathbf{W}, \mathbf{T})) = \begin{cases} \text{true if } \forall j, & \exists i : \delta(\boldsymbol{w}_i, \boldsymbol{t}_j) < 0 \\ \text{false} & \text{otherwise} \end{cases} \tag{8}$$

Equation (8) gives a compact representation of the above two conditions for feasible locators and snap orientations,

$$\text{fully constrained}(\Delta(\bigcup_{k \in L} \mathbf{W}_k, \mathbf{T}_{\text{all}})) = \text{false} \tag{9}$$

$$\text{fully constrained}(\Delta(\bigcup_{k \in L \cup S} \mathbf{W}_k, \mathbf{T}_{\text{all}})) = \text{true} \tag{10}$$

where L and S are the sets of locators and snaps, respectively, $\mathbf{W}_k$ is the wrench matrix of a locator (if $k \in L$) or a snap (if $k \in S$), and $\mathbf{T}_{\text{all}}$ is the twist matrix of all translational motions in $\pm x$, $\pm y$, and $\pm z$ directions,

$$\mathbf{T}_{\rm all}=\begin{pmatrix} 0 & 0 & 0 & 1 & 0 & 0 \\ 0 & 0 & 0 & -1 & 0 & 0 \\ 0 & 0 & 0 & 0 & 1 & 0 \\ 0 & 0 & 0 & 0 & -1 & 0 \\ 0 & 0 & 0 & 0 & 0 & 1 \\ 0 & 0 & 0 & 0 & 0 & -1 \end{pmatrix} \quad (11)$$

Using Eqs. (3) and (4), for example, the virtual coefficient matrix for Fig. 3(*a*) before snap engagement is given as

$$\Delta\Big(\bigcup_{k\in\{l_1,l_2\}}\mathbf{W}_k,\mathbf{T}_{\rm all}\Big)=\begin{pmatrix} 1 & -1 & 0 & 0 & 0 & 0 \\ -1 & 1 & 0 & 0 & 0 & 0 \\ 0 & 0 & 0 & 0 & 1 & -1 \\ 0 & 0 & 1 & -1 & 0 & 0 \\ 0 & 0 & -1 & 1 & 0 & 0 \end{pmatrix} \quad (12)$$

Since the fifth column has no negative entry, fully constrained=false. If $\mathbf{W}_{s1}$ and/or $\mathbf{W}_{s2}$ are added, i.e., if snaps are engaged, the virtual coefficient matrix will have at least one negative entry in each row; thus fully constrained=true. On the other hand, the virtual coefficient matrix for the design in Fig. 3(*b*) after snap engagement is given as

$$\Delta\Big(\bigcup_{k\in\{l_1,l_2\}\cup\{l_1,l_2\}}\mathbf{W}_k,\mathbf{T}_{\rm all}\Big)=\begin{pmatrix} 1 & -1 & 0 & 0 & 0 & 0 \\ -1 & 1 & 0 & 0 & 0 & 0 \\ 0 & 0 & 0 & 0 & 1 & -1 \\ 0 & 0 & 0 & 0 & -1 & 1 \end{pmatrix} \quad (13)$$

Since the matrix does not have negative values in the $+y$ or $-y$ axis, Eq. (10) is not satisfied; i.e., the design is always underconstrained in the y direction.

Since Eqs. (9) and (10) do not prohibit overconstraining of the panel, the same degree of freedom can be constrained by multiple locators and/or snaps. While this may cause undesirable tolerance stack-up, the dimensional tolerances of the panel and frame are assumed to be sufficiently small in the following case study. The issue of overconstrained and tolerance stack-up, however, will be addressed as part of future work.

3.3 Simultaneous Optimization of Locators/Snaps and Heating Areas. In addition to satisfying the motion constraints, an enclosure assembly must satisfy the following thermal and structural requirements:

1. Snaps do not unlock due to the weight of the opposing part in the assembly.
2. Local heating induces displacement sufficient for unlocking the snaps.
3. Uniform heating does not induce displacement sufficient for unlocking all the snaps.
4. Any thermal and structural requirements other than requirement 1 for the desired functions of the product.

Requirement 1 is for preventing accidental disassembly during the normal use of the product. In the optimization problem stated earlier, it is regarded as one of two objective functions to be minimized, together with the total heating area to unlock the snaps. Requirement 2 is for the desired reversal behavior of the locator-snap system. Requirement 3 is for preventing accidental disassembly during the use in an elevated temperature. Examples of requirement 4 include guarding against thermal damage and resonance vibration. Although not explicitly imposed, the use of multiple heating locations can also facilitate the prevention of accidental disassembly in a lock-and-key fashion, which can be observed in some results in the following case study.

The following four design variables are defined for the simultaneous optimization of locators/snaps and heating areas:

- $\boldsymbol{x}=(x_1,x_2,\ldots,x_n)$, where x_i is a vector that identifies the d finite element nodes on edge i on which locators or snaps are placed; x_{ij}=nil if the jth locator/snap is not placed on edge i.
- $\boldsymbol{y}=(y_1,y_2,\ldots,y_m)$, where y_i is a coordinate vector of the four vertices of the ith rectangular area to be heated; y_i=nil if the ith heating area is undefined.
- $\boldsymbol{z}=(c_1,c_2,\ldots,c_n)$, where $c_i=(l_i,o_i)$ is a choice of locator/snap and its orientation of the ith edge as defined in Eq. (2); l_i=nil if the ith edge does not have a locator/snap, in which case the value of o_i is ignored.

Using $\boldsymbol{x}$, $\boldsymbol{y}$, and $\boldsymbol{z}$, the optimization problem can be written as

$$\text{minimize}\{f_1(\boldsymbol{y}),f_2(\boldsymbol{x},\boldsymbol{y},\boldsymbol{z})\}$$

subject to

$$\text{min\_displacement}(\boldsymbol{x},\boldsymbol{y},z) > \boldsymbol{h}_+$$

$$\text{max\_displacement}(\boldsymbol{x},z) < h_-$$

$$\text{structural\_requirements}(\boldsymbol{x},z) = \text{true}$$

$$x_{ij}\in\{\text{nil},L_i,L_i+1,\ldots,U_i\},\quad i=1,\ldots,n,\quad j=1,\ldots,d$$

$$y_i\in P_h^4,\quad i=1,2,\ldots,m$$

$$z\in F$$

where

- $f_1(\boldsymbol{y})$ is the area enclosed by the squares defined in $\boldsymbol{y}$
- $f_2(\boldsymbol{x},\boldsymbol{y},z)$ is the maximum deformation at the mating line under the own weight of the product during snap engagement
- min_displacement $(\boldsymbol{x},\boldsymbol{y},z)$ is the minimum outward steady state thermal displacement of all nodes on which snap-catch pairs are placed when locally heated at temperature T_l in the locations specified by $\boldsymbol{y}$
- max_displacement $(\boldsymbol{x},z)$ is the maximum outward steady state thermal displacement of all nodes on which snap-catch pairs are placed when uniformly heated at temperature $T_u(<T_l)$
- h_+ is the height of snaps plus a small tolerance
- h_- is the height of snaps minus a small tolerance
- structural_requirements $(\boldsymbol{x},z)$ is any structural requirements (other than f_2) during snap engagement
- L_i and U_i are lower and upper bounds of the node numbers of the finite elements on edge i, respectively
- P_h is the feasible region of the heating area
- F is the set of feasible combinations of locators, snaps, orientations, and edges generated as discussed in the previous section.

The evaluation of min_displacement $(\boldsymbol{x},\boldsymbol{y},z)$ and max_displacement $(\boldsymbol{x},z)$ requires thermal-structural FEA, whereas that of $f_2(\boldsymbol{x},\boldsymbol{y},z)$ and structural_requirements $(\boldsymbol{x},z)$ requires structural FEA only.

It should be noted that variables $\boldsymbol{x}$, $\boldsymbol{y}$, and z do not explicitly specify the choice of the part (e.g., top or bottom cover) on which a locator or a protrusion, or similarly a snap or a catch, should be placed. Since the choice does not affect the motion constraints and structural behavior during snap engagement, it can be arbitrary in the case of a locator-protrusion pair. In the case of a snap-catch pair, the choice is determined based on the thermal deformation upon heating. If the surface of a part bulges outward, a catch is placed on the part. If the surface bulges inward, a snap is placed on the part.

Table 1 Material properties of nylon 66–30% glass filled

Property name (units)	Value
Density (g/cm^3)	1.36
Elasticity modulus (MPa)	8500
Poisson ratio	0.36
Melting point (°C)	260
Thermal expansion coefficient (μm/m °C)	30.0
Specific heat capacity (j/kg °C)	1800
Conductivity (W/m K)	0.40

4 Case Study

4.1 Inputs. The proposed method is applied to a DVD player made of two mating pieces of an injection molded nylon 66–30% glass filled enclosure. The DVD player geometry is $250\times 500 \times 150$ mm^3 with a T-shaped mating line and wall thickness of 1.5 mm. The material properties are given in Table 1. Figure 4 shows the simplified model of a case assembly of the DVD player.

Figure 5 shows the FE model of the lower part of the assembly. The mating polygon has eight edges ($n=8$), shown as thick black lines and labeled as $e_1, \ldots, e_8$. The feasible heating region, P_h, is considered as all the eight surfaces of the lower part except its base surface. To facilitate the simplified mapping of the coordinates in $\boldsymbol{y}$ to the heating areas as discussed below, the feasible heating region is subdivided into ten subsurfaces (labeled as $S_{1L}, \ldots, S_{5L}$ and $S_{1R}, \ldots, S_{5R}$), five (5) on each side of the plane of symmetry, as shown in Fig. 5.

4.2 Generation of the Feasible Locator and Snap Orientations. A set of feasible orientations of locator and snaps is precalculated, as discussed earlier. The locator and snap library used in this case study consists of those shown in Figs. 2(*b*) and 2(*d*), and they have the same wrench matrices as in Eqs. (3)–(5). Only the orientations shown in Fig. 3 are considered. After testing all the 256 possible combinations for Eqs. (9) and (10), only 224 are feasible and are included in the feasible set F. In all cases, the assembly direction is to move the two parts toward each other in the z direction in Fig. 4.

4.3 Simultaneous Optimization of Locators and Heating Areas. In order to simplify the specification of heating area by $\boldsymbol{y}$, the feasible heating regions of two symmetric halves of the enclosure are first flattened to rectangular regions as shown in Fig. 6(*a*), and the coordinates in $\boldsymbol{y}$ are then applied on this transformed geometry. Instead of utilizing variable $\boldsymbol{y}$ to explicitly define m heating areas, the case study considers up to two rectangular heating areas by using $\boldsymbol{y}$ with $m=1$ and an auxiliary design variable t defined as

$$t = \begin{cases} 0 & \text{if only left } (L) \text{ side is heated} \\ 1 & \text{if only right } (R) \text{ side is heated} \\ 2 & \text{if both sides are heated} \end{cases} \qquad (14)$$

where the left (L) and right (R) sides are with respect to the surface of symmetry, as defined in Fig. 5. A sample heated area is shown in Fig. 6(*a*), and its equivalent area in the 3D model is shown in Fig. 6(*b*). If $t=0$ instead of 1 in Fig. 6(*b*), the heated area would have been on the other side (gray region).

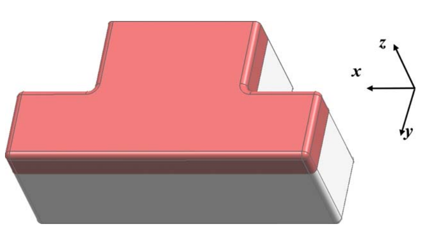

Fig. 4 Simplified model of the case assembly of a DVD player

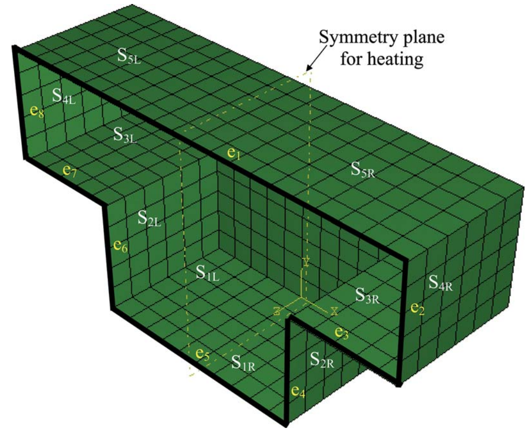

Fig. 5 FE model of the lower part of the assembly showing edges and the feasible heating region

The heating temperatures for local heating and uniform heating are T_l=200°C and T_u=50°C, respectively, in a room at 20°C. During heating, free convection to the air (convection heat transfer coefficient=8 W/m^2 K) is considered as the only source of heat dissipation. It is assumed that each edge can have only one locator or snap ($d=1$).

For the calculation of $f_1(\boldsymbol{y})$, the number of heated nodes is taken as a measure of the heated area. For the calculation of $f_2(\boldsymbol{x},\boldsymbol{y},z)$, a uniformly distributed load of 20 N is applied to the base surface of an enclosure part in $\pm x$, $\pm y$, and $-z$ directions, and the maximum displacement of the nodes on the mating line for all loadings is obtained. A penalty is applied if the minimum displacement of all nodes with snaps under local heating at T_l =200°C is less than $h_+=1$ mm. Since MOGA does not handle constraints explicitly, the minimum displacement constraint is written as a penalty function as follows:

$$f_3(\boldsymbol{x},\boldsymbol{y},z) = \max(0, h_+ - \min\_\text{displacement}(\boldsymbol{x},\boldsymbol{y},z)) \qquad (15)$$

Similarly, a penalty is applied if the maximum displacement of all nodes with snaps under uniform heating T_u=50°C is more than h_-=0.5 mm,

$$f_4(\boldsymbol{x},z) = \max(0, \max\_\text{displacement}(\boldsymbol{x},z) - h_-) \qquad (16)$$

Table 2 shows the GA parameters. Heuristic and arithmetic crossovers are used for all the variables.

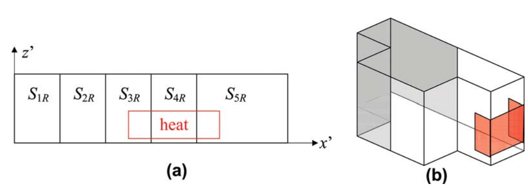

Fig. 6 (*a*) Heating area in the flattened feasible heating subregion S_{1R}–S_{5R} and (*b*) corresponding heating area in 3D

Table 2 GA parameters used in the case study

Parameter	Value
Population size	80
Number of generations	160
Crossover probability	0.95
Mutation probability	0.05

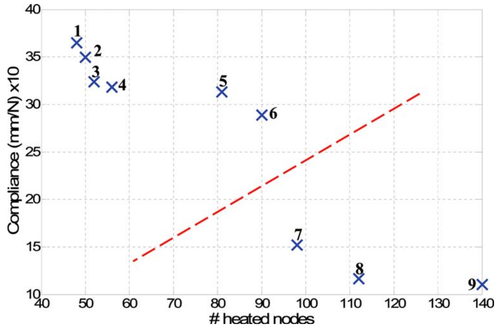

Fig. 7 Pareto-optimal solutions for the case study

4.4 Optimization Results. Figure 7 Shows the Pareto-optimal solutions, which exhibit a trade-off between the part compliance and the amount of heating required (number of heated nodes). The solutions above the dotted line use a single heating area on one side of the DVD ($t=0$ or 1), while the solutions below the line use symmetric heating ($t=2$).

Figure 8 shows the optimal placement of locators and snaps and the response due to local heating of the solution with minimum heating area (solution 1). Locators and snaps are oriented at 0 deg with respect to the surfaces they are attached to. The heating area is 25×575 mm^2 (48 nodes). Locator positions are marked with a black circle, while snap positions are marked with an arrow showing the bulging direction. If the bulging is outward, a catch and a snap are placed on the shown part and the other part (not shown), respectively. The maximum deformation at the mating line under its own weight is due to pressure load in the $+y$ direction at the upper surface and is (0.7292 mm).

Figure 9 shows the optimal placement of locators and snaps and the response due to local heating of an optimum solution with minimum symmetric heating areas (solution 7). Locators and snaps are oriented at 0 deg with respect to the surfaces they are attached to. The heating area is 150 mm$\times$150 mm$\times$2 (98 nodes). The maximum deformation at the mating line under its own weight is due to pressure load in the $-z$ direction at the bottom surface and is (0.3038 mm). If only one side (either left side or right side) is heated, only one snap will unlock while the other snap will remain closed, as shown in Figs. 10(*a*) and 10(*b*). As a result, both sides need to be heated simultaneously to allow unlocking.

Figures 11(*a*) and 11(*b*) and Figs. 12(*a*) and 12(*b*) show computer aided design (CAD) drawings of the top cover and the base part of the final optimized DVD player model for optimum solutions 1 and 7, respectively

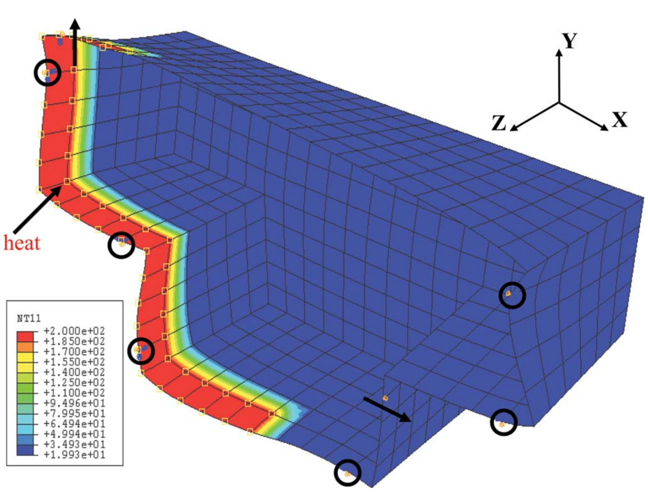

Fig. 8 Optimum solution with minimum heat area (solution 1)

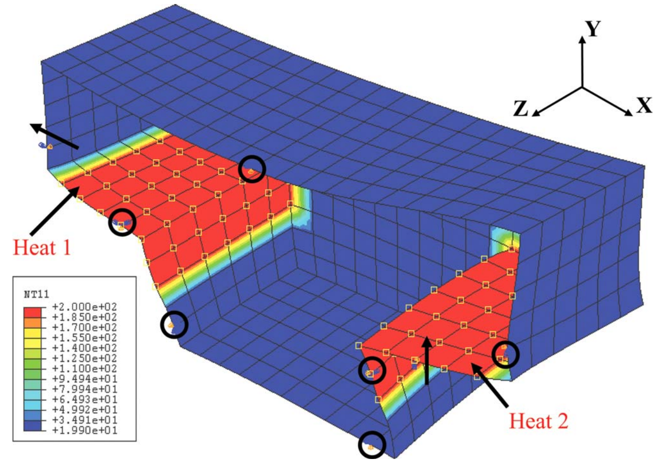

Fig. 9 Optimum solution with minimum symmetric heat area (solution 7)

5 Conclusion and Future Work

This paper presented a unified method for designing a high-stiffness reversible locator-snap system that can be disengaged nondestructively with localized heat while employing normal polymers. The method was applied to a case study on a DVD player enclosure with a T-shaped mating line. The resulting Pareto-optimal solutions exhibit alternative designs with different trade-offs between structural stiffness during snap engagement

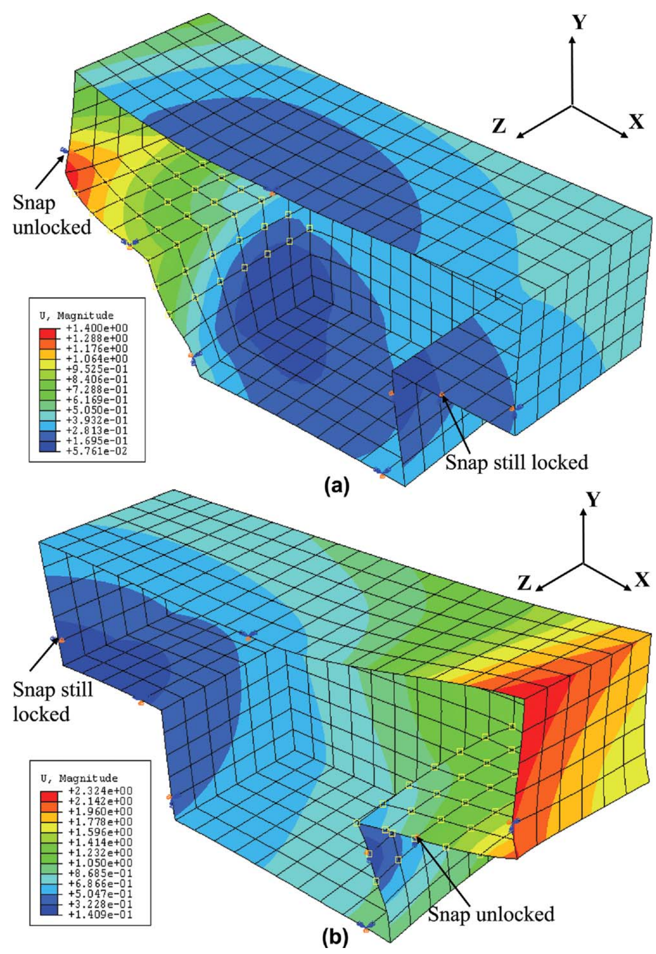

Fig. 10 Solution 7 response to one sided heating: (*a*) area 1 is heated and (*b*) area 2 is heated

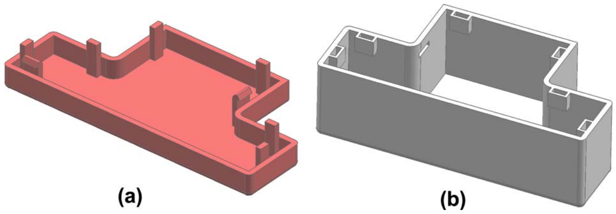

Fig. 11 CAD drawing for the optimized DVD player model (solution 1): (*a*) top part and (*b*) base part

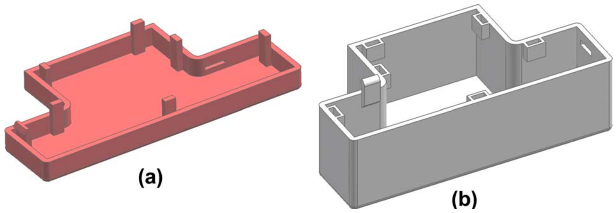

Fig. 12 CAD drawing for the optimized DVD player model (solution 7): (*a*) top part and (*b*) base part

and heating area necessary for snap disengagement. Some results require simultaneous heating of two areas, demonstrating the idea of a lock-and-key.

Future work includes the explicit inclusion of a lock-and-key separation into the problem formulation, addressing the issue of undesired tolerance stack-up due to the use of multiple locators, reviewing the ANSI/IEC standards to find lower limit values for the enclosure stiffness and including these values as design constraints, studying the impact of using variable/flexible mating lines where different mating lines can be examined prior to optimization and where the best mating line is considered during optimization, and extending the problem formulation to generic 3D geometries, relaxing some or all assumptions made in the present study.

References

[1] Boothroyd, G., and Alting, L., 1992, "Design for Assembly and Disassembly," CIRP Ann., **41**, pp. 625–636.

[2] Jovane, F., Alting, L., Armillotta, A., Eversheim, W., Feldmann, K., and Seliger, G., 1993, "A Key Issue in Product Life Cycle: Disassembly," CIRP Ann., **42**, pp. 651–658.

[3] Keoleian, G., and Menerey, D., 1994, "Sustainable Development by Design: Review of Life Cycle Design and Other Approaches," Air Waste, **44**(5), pp. 645–668.

[4] Gungor, A., and Gupta, S., 1999, "Issues in Environmentally Conscious Manufacturing and Product Recovery: A Survey," Comput. Ind. Eng., **36**(4), pp. 811–853.

[5] Koch, P., "Snap Fit Design," The Pennsylvania State University, Eire, PA, http://engr.bd.psu.edu/pkoch/plasticdesign/snap_design.htm.

[6] Ball, R. S., 1900, *A Treatise on the Theory of Screws*, Cambridge University Press, Cambridge, UK.

[7] Coello, C., Veldhuizen, D., and Lmont, G., 2002, *Evolutionary Algorithms for Solving Multi-Objective Problems*, Kluwer Academic, Dordrecht, MA.

[8] Deb, K., Pratap, A., Agarwal, S., and Meyarivan, T., 2002, "A Fast and Elitist Multiobjective Genetic Algorithm: NSGA-II," IEEE Trans. Evol. Comput., **6**(2), pp. 182–197.

[9] Shetty, D., Rawolle, K., and Campana, C., 2000, "A New Methodology for Ease-of-Disassembly in Product Design," Recent Advances in Design for Manufacture (DFM); presented at the 2000 ASME International Mechanical Engineering Congress and Exposition, November 5–10, Orlando, FL, pp. 39–50.

[10] Suri, G., and Luscher, A., 1999, "Structural Abstraction in Snap-Fit Analysis," *Proceedings of the 1999 ASME Design Engineering Technical Conferences*, Las Vegas, NV, Sept. 12–15, Paper No. DETC1999/DAC-8567.

[11] Nichols, D., and Luscher, A., 1999, "Generation of Design Data Through Numerical Modeling of a Post and Dome Feature," *Proceedings of the 1999 ASME Design Engineering Technical Conferences*, Las Vegas, NV, Sept. 12–15, Paper No. DETC1999/DAC-8596.

[12] Turnbull, V., 1984, "Design Considerations for Cantilever Snap-Fit Latches in Thermoplastics," *Proceedings of the Winter Annual Meeting of ASME*, New Orleans, LA, Paper No. 84-WA/Mats-28, pp. 1–8.

[13] Wang, L., Gabriele, G., and Luscher, A., 1995, "Failure Analysis of a Bayonet-Finger Snap-Fit," *Proceedings of the ANTEC '95*, Boston, MA, May, pp. 3799–3803.

[14] Larsen, G., and Larson, R., 1994, "Parametric Finite-Element Analysis of U-Shaped Snap-Fits," *Proceedings of the ANTEC '94*, San Francisco, CA, pp. 3081–3084.

[15] Genc, S., Messler, R., Bonenberger, P., and Gabriele, G., 1997, "Enumeration of Possible Design Options for Integral Attachment Using a Hierarchical Classification Scheme," ASME J. Mech. Des., **119**, pp. 178–184.

[16] Genc, S., Messler, R., Jr., and Gabriele, G., 1998, "A Systematic Approach to Integral Snap-Fit Attachment Design," Res. Eng. Des., **10**, pp. 84–93.

[17] Genc, S., Messler, R., Jr., and Gabriele, G., 1998, "A Hierarchical Classification Scheme to Define and Order the Design Space for Integral Snap-Fit Assembly," Res. Eng. Des., **10**, pp. 94–106.

[18] Luscher, A., Suri, G., and Bodmann, D., 1998, "Enumeration of Snap-Fit Assembly Motions," *Proceedings of the ANTEC '98*, pp. 2677–2681.

[19] Chiodo, J., Jones, N., Billett, E., and Harrison, D., 2002, "Shape Memory Alloy Actuators for Active Disassembly Using 'Smart' Materials of Consumer Electronic Products," Mater. Des., **23**, pp. 471–478.

[20] Li, Y., Saitou, K., Kikuchi, N., Skerlos, S., and Papalambros, P., 2001, "Design of Heat-Activated Reversible Integral Attachments for Product-Embedded Disassembly," *Proceedings of the EcoDesign 2001: Second International Symposium on Environmentally Conscious Design and Inverse Manufacturing*, Tokyo, Japan, Dec. 12–15, pp. 360–365.

[21] Li, Y., Saitou, K., and Kikuchi, N., 2003, "Design of Heat-Activated Reversible Integral Attachments for Product-Embedded Disassembly," International Journal of CAD/CAM, **3**, pp. 26–40.

[22] Li, Y., Saitou, K., and Kikuchi, N., 2003, "Design of Heat-Activated Compliant Mechanisms for Product-Embedded Disassembly," Proceedings of the Fifth World Congress on Computational Mechanics, Vienna, Austria, Jul. 7–12.

[23] Shalaby, M., and Saitou, K., 2005, "Design of Heat Reversible Snap Joints for Space Frame Bodies," Proceedings of the ASME Design Engineering Technical Conferences, Long Beach, CA, Sept. 24–28, Paper No. DETC2005-85155.

[24] Shalaby, M., and Saitou, K., 2006, "Optimal Heat-Reversible Snap Joints for Frame-Panel Assembly in Aluminum Space Frame Automotive Bodies," Proceedings of the 13th CIRP International Conference on Life Cycle Engineering, LCE2006, Leuven, Belgium, May 31–Jun. 2.

[25] Waldron, K. J., 1966, "The Constraint Analysis of Mechanisms," J. Mech., **1**(2), pp. 101–114.

[26] Konkar, R., and Cutkosky, M., 1995, "Incremental Kinematic Analysis of Mechanisms," ASME J. Mech. Des., **117**, pp. 589–596.

[27] Adams, J. D., and Whitney, D. E., 1999, "Application of Screw Theory to Constraint Analysis of Assemblies of Rigid Parts," Proceedings of the 1999 IEEE International Symposium on Assembly and Task Planning, Porto, Portugal, July 2–24, pp.69–74.

[28] Adams, J. D., and Whitney, D. E., 1999, "Application of Screw Theory to Motion Analysis of Assemblies of Rigid Parts," Proceedings of the 1999 IEEE International Symposium on Assembly and Task Planning, Porto, Portugal, July 21–24, pp.75–80.

[29] Lee, B., and Saitou, K., 2006, "Three-Dimensional Assembly Synthesis for Robust Dimensional Integrity Based on Screw Theory," ASME J. Mech. Des., **128**, pp. 243–251.